445580 N/S

NNGW-2898

IN-74-CR

191269

19 P

Design and fabrication of a reflection far ultraviolet polarizer and retarder

Jongmin Kim, Muamer Zukic, Michele M. Wilson, and Douglas G. Torr

Department of Physics, The University of Alabama in Huntsville
Optics Building, Suite 300, Huntsville, AL. 35899

ABSTRACT

New methods have been developed for the design of a far ultraviolet multilayer reflection polarizer and retarder. A MgF_2/Al/MgF_2 three-layer structure deposited on a thick opaque Al film (substrate) is used for the design of polarizers and retarders. The induced transmission and absorption method is used for the design of a polarizer and layer-by-layer electric field calculation method is used for the design of a quarterwave retarder. In order to fabricate these designs in a conventional high vacuum chamber we have to minimize the oxidation of the Al layers and somehow characterize the oxidized layer. X-ray photoelectron spectroscopy is used to investigate the amount and profile of oxidation. Depth profiling results and a seven layer oxidation model are presented.

1. INTRODUCTION

In the far ultraviolet (FUV : 120 ~ 230 nm) region, a MgF_2 crystal is known to be birefringent down to 130 nm,[1] and has been used as a transmission polarizer.[2,3] Some authors used LiF[4] and MgF_2,[5] crystals for a reflection polarizer. Complete polarization is achieved when a transparent crystal is oriented at its Brewster angle, but metal surfaces have higher reflectances than crystals.[6] A single metal surface at the Pseudo-Brewster angle of incidence is not enough for a high degree of polarization, and Hamm et. al.[7] designed a triple-reflection-polarizer (TRP) using gold coated mirrors.

It is known that in the FUV region a LiF and MgF_2 crystal can act as a retarder when pressure is applied to the edges of the crystal.[1] There also have been studies on the use of metallic surfaces as quarterwave retarders (QWR).[5,8] The authors adjusted the angle representing the orientation of the electric vector of the incident photon beam with respect to the plane of incidence to make the reflectances equal for both polarization states.

We have reported three-layer thin film design methods for a FUV polarizer[9] and a QWR.[10] As coating materials we use MgF_2 and Al. The polarizer design is based on the known effect of induced transmission and absorption in high-low absorbing multilayer structures. The induced transmission/absorption approach provides an effective means of attaining the absolute maximum reflection ratio of s- to p-polarization on a layer-by-layer basis and also gives clear insight into the evaluation of the s- and p- amplitude reflectance and transmittance through a polarizer. Similarly, the knowledge about the phase difference between s- and p-polarization on a layer-by-layer basis provides an excellent design method for multilayer reflection QWRs.

Oxidation of an Al layer in a conventional high vacuum chamber (~10⁻⁶ torr) is a serious problem which has to be solved for successful fabrication of polarizer and QWR designs. Obviously, the problem is easily solved if the designs were fabricated in an ultrahigh vacuum (UHV) coater (~10⁻¹⁰ torr). Since we do not have access to an UHV system, we need to understand the Al oxidation process. The experimental and theoretical techniques for modeling of Al oxidation in the polarizer and QWR designs are explained.

2. DESIGN METHODS

2.1. FUV polarizer design

The coating materials used are MgF_2, a very low absorbing FUV material, and Al, a very high absorbing FUV material. Fresnel coefficients are quite different between s- and p-polarizations for oblique angles of incidence at the boundaries of these materials. This property is used to achieve a large difference in reflectance between the two polarizations.

Berning and Turner[11] showed that a reasonably thick metal film can be induced to transmit a surprising amount of energy of a particular wavelength when it is surrounded by suitably chosen interference film combinations. They called this technique 'induced transmission' and applied it to a bandpass filter design. A polarizer can be designed by inducing transmission and absorption for p- while maintaining a large reflectance for s-polarization.[9]

Consider now a MgF_2/Al/MgF_2 three-layer structure which together with an Al substrate provides 3 high-low absorptance boundaries. The top MgF_2 layer thickness is determined to make the p-polarization amplitude a minimum when it enters into the central Al layer. Then the p-polarization light passes through the central Al layer with very little absorption. The bottom MgF_2 layer works as a transmission and absorption induced layer. This layer makes the p-polarization amplitude large when it goes back to the central Al layer and when it transmits into the Al substrate. This layer increases both reflected and transmitted p-polarization electric field amplitudes at the MgF_2/Al boundaries. Therefore, antireflective properties of the bottom MgF_2 layer induce transmission and absorption of the p-electric field in the middle and bottom (substrate) Al layer. Both Al layers absorb p-polarized light and therefore reduce p-reflection of the MgF_2/Al/MgF_2 design. Since the polarizer is designed as a p-polarization trap and the s-polarization is affected differently, the s-polarized light is reflected from the 3-layer structure with little loss. Figure 1 shows the calculated s and p spectral reflectance of a polarizer designed for 130.4 nm and at a 45° angle of incidence. The calculated reflectance for s-polarization is 92.7% while p-polarized light reflectance is less than 0.001%.

2.2. FUV quarterwave retarder design

A QWR takes advantage of the same three-layer structure used for the polarizer design.[10] In this case the difference in Fresnel coefficients is used to achieve a phase difference. A multilayer that satisfies the following requirement imposed on amplitude reflectances and phases is known as a QWR.

$$\frac{r_s}{r_p} = \pm \; i \qquad\qquad\qquad (1)$$
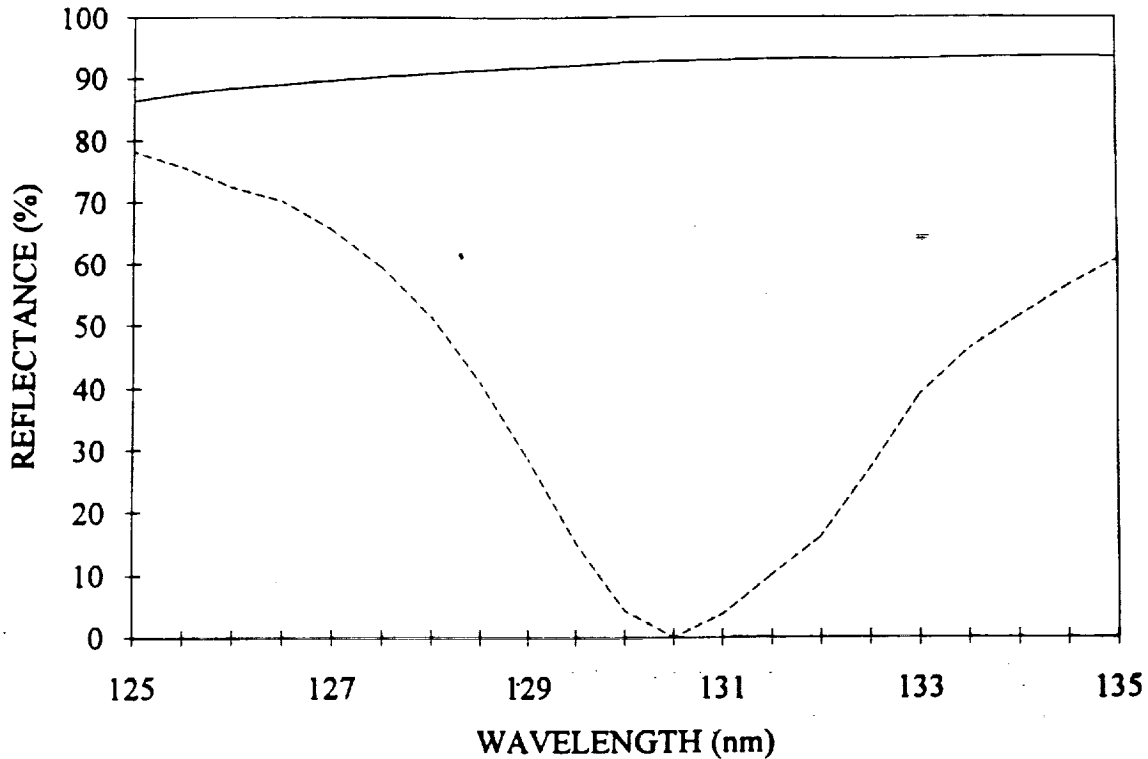
Figure 1. Calculated reflectance for s-polarization (solid line) and p-polarization (dashed line) of a polarizer designed for 130.4 nm and a 45° angle of incidence.

In addition to the basic requirement given above, a QWR needs to have a high reflectance for both polarization states. Therefore, the central Al layer should be as thin as possible to avoid large losses due to absorption. The design task then becomes that of determining the thickness of the two MgF$_2$ layers that will yield the best performance.

At the first boundary, the incident amplitude is 1, and the reflected amplitudes for s- and p-polarizations are decided by the target reflectance and basic QWR requirement given by Eq. (1). Starting with these two electric fields, the fields at the top of the 4th boundary can be calculated. In addition these two fields are related by the Fresnel reflection coefficients, thus providing a system of two equations with two unknowns; one for each polarization state

Vacuum   Boundary

		1
MgF_2	ϕ_1	
		2
Al	δ	
		3
MgF_2	ϕ_2	
		4
Al substrate		
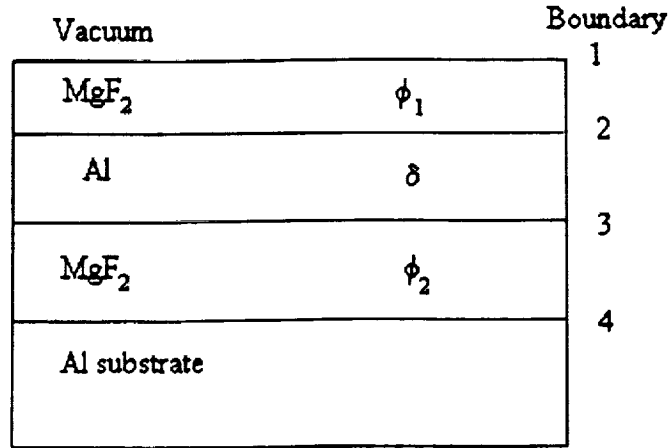
Figure 2. Schematic diagram of the QWR structure to show the notation of the thickness and number of boundaries.

$$e^{i(\phi_1+\phi_2)}(r_{s/p}-r_{12})(e^{i\delta}-r_{23}^{2}e^{-i\delta})$$
$$+e^{-i(\phi_1+\phi_2)}(1-r_{s/p}r_{12})(r_{23}^{3}e^{i\delta}-r_{23}e^{-i\delta})$$
$$+e^{i(\phi_1-\phi_2)}(r_{s/p}-r_{12})r_{23}^{2}(e^{-i\delta}-e^{i\delta})$$
$$+e^{-i(\phi_1-\phi_2)}(1-r_{s/p}r_{12})r_{23}(e^{-i\delta}-e^{i\delta})=0$$

(2)

where $r_{s/p}$ is the target amplitude reflectance for the s- and p-polarizations, r_{12} and r_{23} are the Fresnel reflection coefficients at the vacuum/MgF_2 boundary and the MgF_2/Al boundary, respectively, and δ is the phase thickness of the central Al layer. The two unknowns, ϕ_1 and ϕ_2 are the phase thicknesses of the two MgF_2 layers.

Figure 3 shows a QWR designed for 130.4 nm that has 89.09 % reflectance for the s-polarization and 89.11 % for the p-polarization state. The phase difference between these two polarization states is 90.04°. For convenience the QWR is designed for a 45° angle of incidence, but our design approach can be used for any other angle of incidence.

3. OXIDATION PROBLEM OF ALUMINUM LAYERS

We fabricated a polarizer which was expected to have reflectances as shown in Figure 1. The deposition was done in a vacuum of 1.9X10^{-6} torr. The measured performance was quite different from the design values as is shown in Figure 4. We assume that our coated Al layers have different optical constants from the values we used for design. In the design, we used Al optical constants obtained for films produced in ultrahigh vacuum, from reference 12. But an ultrahigh vacuum chamber is not available to us and it is known that Al oxidizes even in high vacuum. We have to minimize the oxidation using

our conventional high vacuum chamber (~10^{-6} torr) and characterize our Al film, which would have different optical constants from those used in the design.

The oxidation problem of the Al layer has been studied by many methods[13-19] and here we summarize the commonly known facts.

- Generally, the higher the vacuum and the faster the evaporation, the higher the reflectance of the Al mirror.
- A surface oxide of an Al film does not strongly effect the reflectance down to 180 nm, but at the shorter wavelengths of the FUV the oxide layer decreases the reflectance significantly.
- The films produced in ultrahigh vacuum (10^{-9}~10^{-10} torr) are believed to correspond to an uncontaminated Al surface.
- The films evaporated in conventional high vacuum are more-or-less oxidized.

In order to minimize the oxidation, we have to deposit the Al film very fast and we cover it with MgF_2 in a minimum time. Halford et. al.[16] reported that if the pressure to deposition rate ratio is smaller than 10^{-8} ~10^{-9} torr min./A° the film has pure Al properties. For the Al substrate case, we can deposit as fast as possible. But for the central Al layer, we have to deposit slowly to control the thickness exactly. Therefore, our two Al layers are expected to have different oxidation properties.
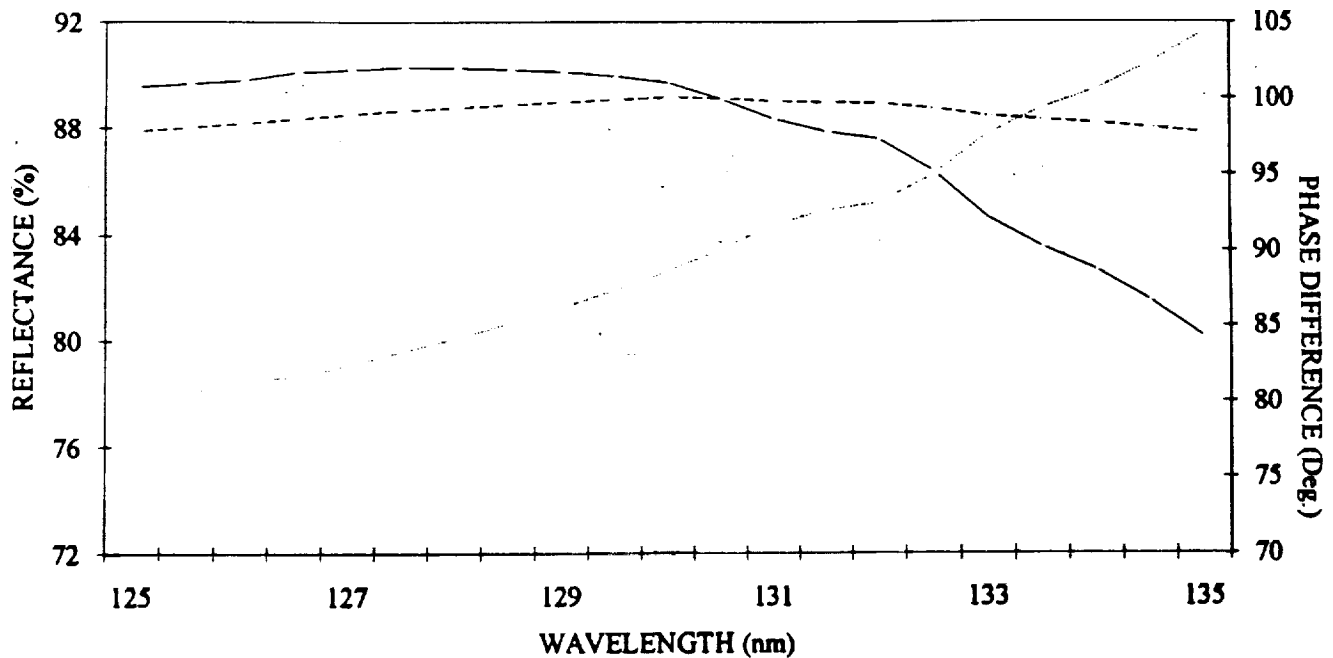
Figure 3. Calculated reflectances for s-polarization (long-dashed line) and p-polarization (short-dashed line), and the phase difference (dotted line) between the two polarizations of a QWR designed for 130.4 nm at a 45° angle of incidence.
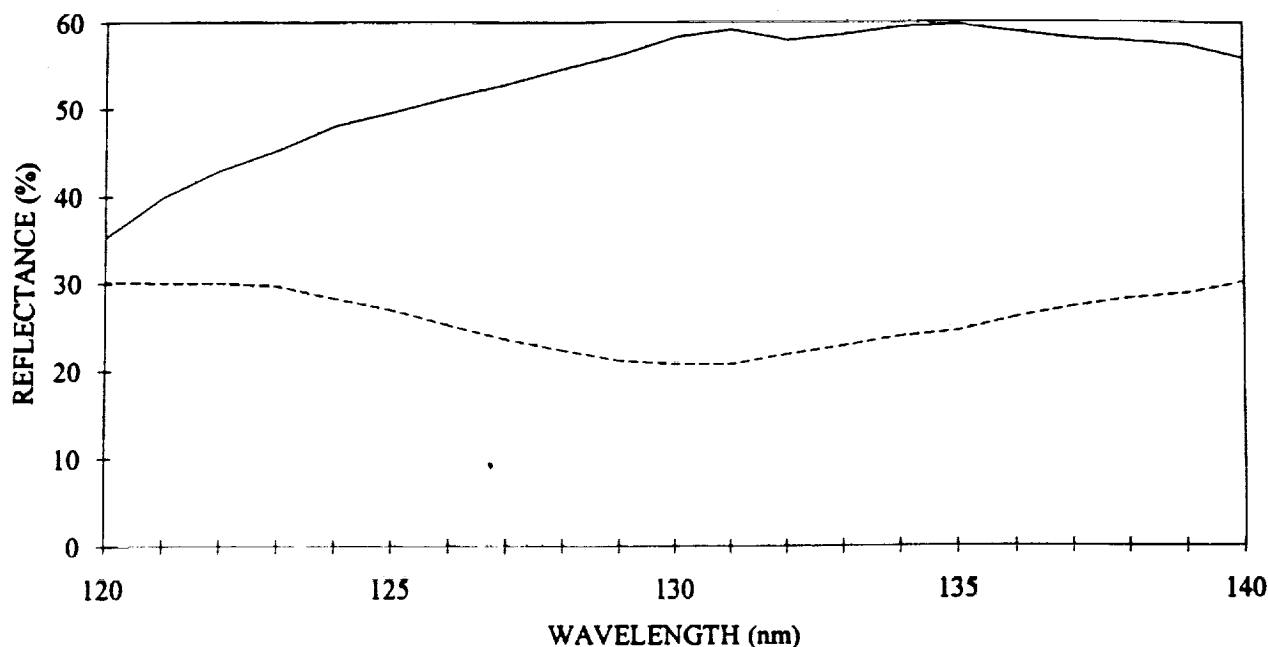
Figure 4. Measured s-(solid line) and p-polarization(dashed line) reflectances of a polarizer designed as Figure 1.

4. DEPTH PROFILING ANALYSIS

In order to understand the oxidation characteristics of our Al films we tried to take a picture of the actual thin film structure using the x-ray photoelectron spectroscopy (XPS) depth profiling method.[20] XPS is a widely used analytical ultrahigh vacuum technique for investigating the chemical composition of solid surfaces. With this XPS system we illuminate the thin film surface with the Mg (or Al) K-α line x-rays and analyze the photo electrons and Auger electrons coming out of the surface. The typical output of an XPS experiment shows the number of electrons as a function of binding energy. Therefore, the position of a peak detects the presence of an element in the surface, and the height of a peak is proportional to the concentration of the element. The XPS system can calculate the concentration of an element from the area and the sensitivity of the peak.[21]

Figure 5 shows the oxidation of the Al substrate layer as one of our depth profiling analysis results for a sample of MgF_2(25 nm)/Al(92 nm) deposited on a Pyrex substrate in a vacuum of 5.0×10^{-6} torr. Al and MgF_2 layers are deposited at a rate of 4.4 nm/sec. and 0.2 nm/sec., respectively, and there is a 7 seconds time delay switching between material.

Our Ar ion gun is not calibrated so Figure 5 shows the volume concentration as a function of etch time. According to this figure we reach the boundary of MgF_2/Al and Al/Pyrex in about 13 minutes and 70 minutes, and this corresponds to etching MgF_2 and Al at a rate of 1.92 nm/min. and 1.61 nm/min., respectively.

The top figure shows that the bottom part of the Al layer is not oxidized thanks to our fast deposition, but during the material switching time the top surface is oxidized down an 8 nm thickness, and MgF_2 has some oxygen in it. It also shows that magnesium and silicon are interdiffused into the Al layer.

The bottom figure shows the contaminants concentration. It shows that in spite of our careful sample preparation and handling, our Pyrex and MgF_2 surfaces are contaminated by carbon. It also shows that we have a sodium contaminant of 2.5% in our MgF_2 layer. We cannot explain the origin of this contamination. (The purity of our coating material is 99.95 %.) The XPS is a very complicated system and there is some possibility of misinterpretation. Therefore, this result is still open to question. We are going to continue this experiment and try to explain the origin of these contaminants and also their effect on the film performance.

We will also try the same analysis for a MgF_2/Al sample deposited at a slow rate which we can control thickness exactly to find out the oxidation property of the central Al layer. The measured profile in Figure 5 is a result of the convolution of the true profile and resolution function of the system. If we deconvolve the resolution function we can have a sharper boundary profile. Then we will have a better idea about the thickness of the oxidized Al.

5. TECHNIQUES FOR MODELING AND CHARACTERIZATION OF THE ALUMINUM LAYER

We plan to analyze these results in the following way. From the depth profiling analysis results in Figure 5, we conclude that the Al substrate can be modeled as two different sublayers - an oxidized Al layer (about 8 nm thickness) on the thick opaque Al substrate. From the reflectance measurements of this MgF_2/Al oxide/Al structure for different incident angles or for different MgF_2 layer thicknesses, we will try to characterize our oxidized Al layer by optical constants. For the bottom part of Al, the reported optical constants in reference 12 will be used as the starting point. If interdiffused elements, Si and Mg, do not have a significant effect, the bottom part of the Al has similar optical constants as pure Al. If the interdiffused elements change the property of Al much we may need many more measurements and numerical fitting of the optical constants.

The central Al layer will be characterized using a similar procedure. First of all we will fabricate the samples using the appropriate deposition rate, which can be repeatedly deposited during fabrication for the control of the exact thickness. Then we will analyze the depth profile by the XPS experiment. We anticipate that the layer can be modeled as three different sublayers. At the moment we open the shutter the Al molecules which travel to the substrate will combine with oxygen molecules remaining in the vacuum chamber. The Al molecules which reach the substrate later will have less of a chance to meet oxygen than the first arriving ones. And during the material switching time the top layer will be oxidized similar to the substrate Al case. Therefore, our fabricated polarizer and QWR are expected to have a seven layer structure as shown in Figure 6.
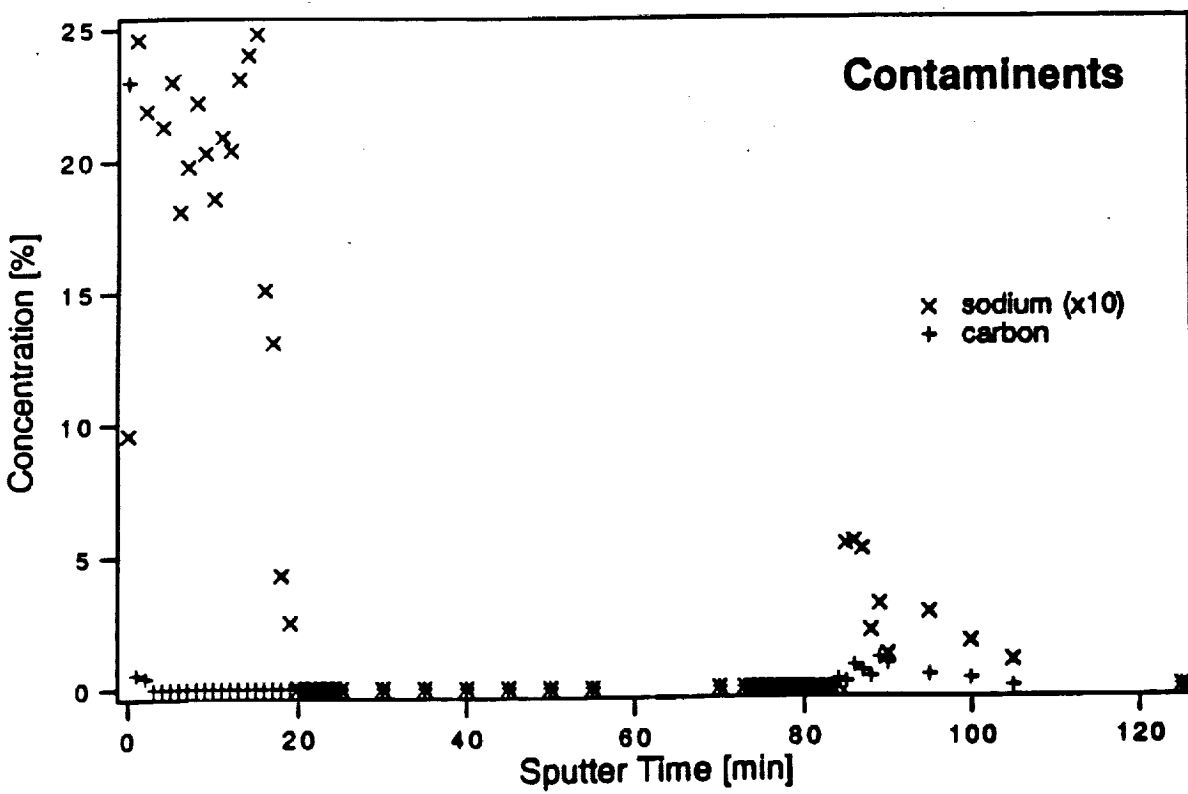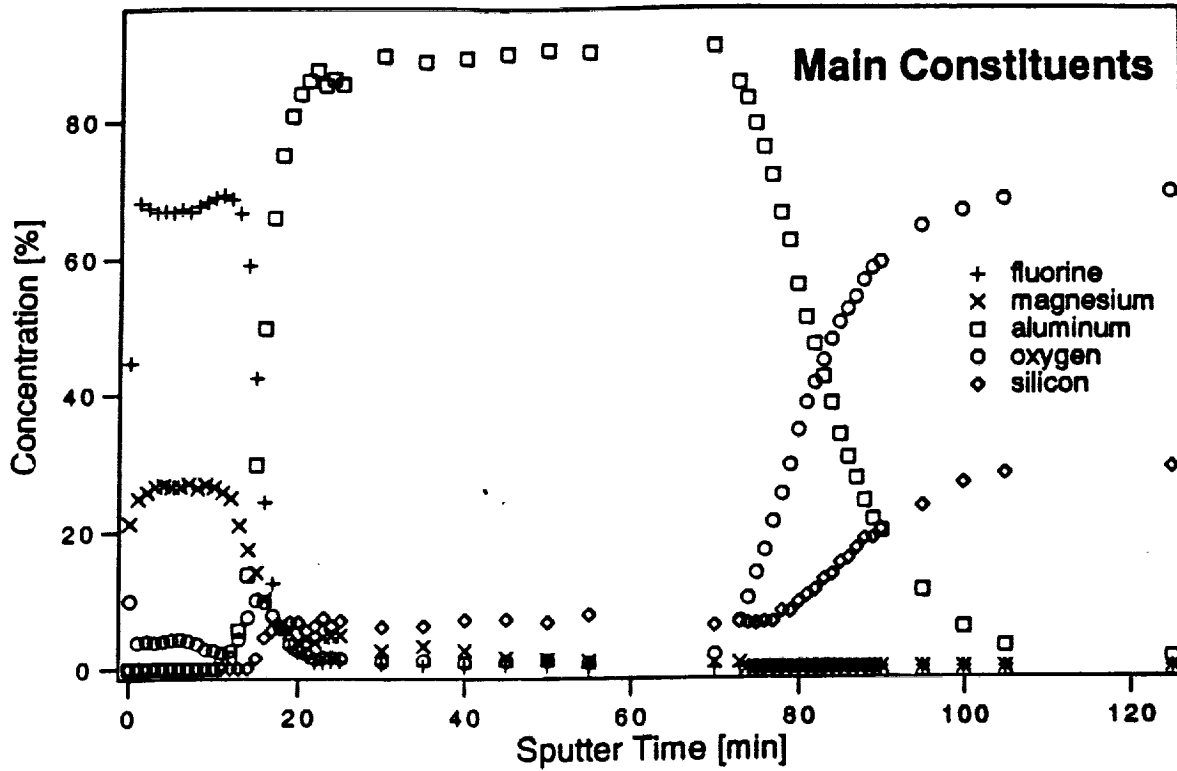
Figure 5. Result of depth profiling analysis using an XPS system for a MgF_2/Al structure. The top is for main constituents and bottom is for contaminants.

MgF$_2$
Oxidized Al #1
Oxidized Al #2
Oxidized Al #3
MgF$_2$
Oxidized Al #4
Al substrate
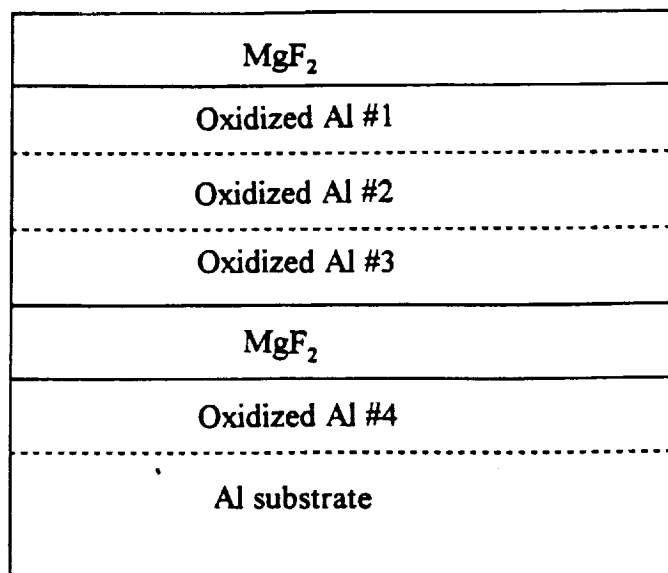
Figure 6. Schematic diagram of the 7-layer oxidation model of the MgF$_2$/Al/MgF$_2$ on an Al substrate. The different numbers of the oxidized Al means that they are oxidized differently.

The depth profiling analysis will give us ideas about the thickness and volume concentration of oxygen for these possible sublayers. Comparing the amount of oxygen and the reflectance measurements, a mathematical fitting method will be used to determine the optical constants of these layers.

Using the optical constants and thicknesses of the Al sublayers, we will optimize the thickness of the two MgF$_2$ layers. During the fabrication of this revised design we will maintain all deposition parameters to obtain the same Al sublayers.

6. SUMMARY

A MgF$_2$/Al/MgF$_2$ three-layer structure on opaque Al is found very useful for designing a FUV polarizer and QWR. For thickness determination we use the induced transmission and absorption method for the polarizer and a layer-by-layer electric field calculation method for the QWR. In order to fabricate these three-layer structures in a conventional vacuum, we need to minimize the oxidation of the Al layer and characterize the oxidized Al layer. For the characterization we propose a 7-layer oxidation model. The XPS depth profiling analysis can be used for the determination of the thickness and oxidation amount of the Al layer.

7. ACKNOWLEDGMENTS

XPS experiments. The first author would like to thank the Agency for Defense Development of Korea and the Physics Department of UAH for the graduate student assistantship received during this study.

8. REFERENCES

1. J. A. R. Samson, **Techniques of Vacuum Ultraviolet Spectroscopy**, chap. 9, John Wiley & sons, New York, 1967.
2. W. C. Johnson, "Magnesium fluoride polarizing prism for the vacuum ultraviolet", Rev. Sci. Instrum., 35, pp. 1375, 1964.
3. H. Winter and H. W. Ortjohann, "High transmission polarization analyzer for Lyman-α radiation", Rev. Sci. Instrum., 58, pp. 359, 1987.
4. T. J. McIlrath, "Circular polarizer for Lyman-α flux", J. Opt. Soc. Am., 58, pp. 506, 1968.
5. T. Saito, A. Ejiri, and H. Onuki, "Polarization properties of an evaporated aluminum mirror in the VUV region", Appl. Opt., 29, pp. 4538, 1990.
6. G. Hass and W. R. Hunter, " Reflection polarizers for the vacuum ultraviolet using Al + MgF$_2$ plate", Appl. Opt., 17, pp. 76, 1978.
7. R. N. Hamm, R. A. MacRae, and E. T. Arakawa, "Polarization studies in vacuum ultraviolet", J. Opt. Soc. Am., 55, pp. 1460, 1965.
8. W. B. Westerveld, K. Becker, P. W. Zetner, J. J. Corr, and J. W. McConkey, "Production and measurement of circular polarization in VUV", Appl. Opt., 24, pp. 2256, 1985.
9. J. Kim, M. Zukic, and D. G. Torr, "Multilayer thin film designs as far ultraviolet polarizers", in **Multilayer and Grazing Incidence X-Ray/EUV Optics for Astronomy and Projection Lithography**, R. B. Hoover and A. B. C. Walker, Jr., ed., Proc. SPIE, Vol. 1742, pp. 413, 1992.
10. J. Kim, M. Zukic, M. M. Wilson, and D. G. Torr, "Multilayer thin film designs as far ultraviolet quarterwave retarders", in **Multilayer and Grazing Incidence X-Ray/EUV Optics for Astronomy and Projection Lithography**, R. B. Hoover and A. B. C. Walker, Jr., ed., Proc. SPIE, Vol. 1742, pp. 403, 1992.
11. P. H. Berning and A. F. Turner, "Induced transmission in absorbing films applied to band pass filter design", J. Opt. Soc. Am., 47, pp. 230, 1957.
12. Y. D. Smith, E. Shiles, and M. Inokuti, "The optical properties of metallic aluminum", in **Handbook of Optical Constants of Solids**, E. D. Palik ed., Academic Press, Orlando, 1985.
13. G. Hass, "Filmed Surfaces for Reflecting Optics", J. Opt. Soc. Am., 45, pp. 945, 1955.
14. G. Hass and J. E. Waylonis, "Optical Constants and Reflectance and Transmittance of Evaporated Aluminum in the Visible and Ultraviolet", J. Opt. Soc. Am., 51, pp. 719, 1961.
15. L. R. Canfield, G. Hass, and J. E. Waylonis, "Further studies on MgF$_2$ - Overcoated Aluminum Mirrors with Highest Reflectance in the Vacuum Ultraviolet", Appl. Opt., 5, pp. 45, 1966.
16. J. H. Halford, F. K. Chin, and J. E. Norman, "Effects of vacuum deposition conditions on ellipsometric parameters, optical constants, and reflectance of ultrapure aluminum films", J. Opt., Soc. Am., 63, pp. 786, 1973.
17. P. B. Barna, Z. Bodo, G. Gergery, D. Szigethy, J. Adam, and P. Jakab, "Electron microscopic and ellipsometric studies on oxidized aluminum layers", Vacuum, 33, pp. 93, 1983.
18. E. Fonana, R. H. Pantell, and M. Moslehi, "Characterization of dielectric-coated metal mirrors using surface plasmon spectroscopy", Appl. Opt., 27, pp. 3334, 1988.
19. Z. Bodo and G. Gergely, "Intrinsic optical constants of aluminum", Appl. Opt., 26, pp. 2065, 1987.

20. S. Hofmann, "Depth Profiling in AES and XPS", in **Practical Surface Analysis**, 2nd. ed., Vol. 1, D. Briggs and M. P. Seah ed., ch. 4, Wiley, Chichester, 1990.

21. C. D. Wagner, W. M. Riggs, L. E. Davis, J. F. Moulder, and G. E. Muilenberg, **Handbook of x-ray photoelectron spectroscopy**, Perkin-Elmer, 1978.

Transparent conductive coatings
in the far ultraviolet

Jongmin Kim, Muamer Zukic, Jung Ho Park, Michele M. Wilson,
Charles E. Keffer, and Douglas G. Torr

Department of Physics, The University of Alabama in Huntsville
Optics Building, Suite 300, Huntsville, AL. 35899

ABSTRACT

In certain cases a space-borne optical instrument with a dielectric window requires a transparent conductive coating deposited on the window to remove the electrostatic charge collected due to the bombardment of ionized particles. Semiconductor and metal films are studied for use as transparent conductive coatings for the front window of far ultraviolet camera. Cr is found to be the best coating material. The theoretical search for the semiconductor and metal coating materials and experimental results for ITO and Cr films are reported.

1. INTRODUCTION

Some optical instruments flown on orbiting satellites have exterior dielectric windows. Due to bombardment by ionized particles, electrostatic charge accumulates on the window which may cause undesirable effects. This prompted investigation into the properties of a conductive transparent coating for use as a surface layer to remove the undesirable electrostatic charges.

Transparent conductive coatings combine high optical transmission with good electrical conductivity and have a number of interesting applications : liquid crystal and gas discharge displays, front electrodes for solar cells, heating stages for optical microscopes, IR reflectors, photoconductors in television camera vidicons, Pokell cells for laser Q-switches, and antistatic coatings.

Combining the properties of transparency and conductivity in the same coating material is not trivial and is only possible with certain semiconductors and with very thin and very low electrically resistant metal films. Thin metal films are widely applied as IR reflectors, but are not extensively used as transparent semiconductors.[1] In general, semiconducting oxides exhibit better electrical and optical properties than thin metal films. Also, metal films are not very resistant to abrasion and other forms of mechanical damage.

For applications in which transparency is much more important than electrical conductivity, SnO_2 is usually employed because its absorption edge occurs further into the UV than other oxide materials. In other classes of devices, in which transparency must be sacrificed for maximum conductivity, indium tin oxide (ITO) (In_2O_3:Sn) is ordinarily used because it yields the highest conductivity and because it can be etched easily.[1]

So far studies about transparent conductive coatings have focused only on the visible and IR regions. In the far ultraviolet (FUV) region, all optical materials are absorbing and reflection optics have been widely used. Therefore, a transparent conductive coating in the FUV region is a new problem to be addressed. Published materials for transparent conductive coatings in the visible and IR region were reviewed by Holland[2] in 1958 and Vossen[1] in 1977. These papers served as a starting point in our research to find FUV transparent conductive coatings.

2. INSTRUMENTAL REQUIREMENTS

The FUV imager[3] for the International Solar Terrestrial Physics (ISTP) mission is designed to image four features of the aurora : O I lines at 130.4 nm and 135.6 nm and the N_2 Lyman-Birge-Hopfield (LBH) bands between 140 nm ~160 nm (LBH short) and 160 nm ~180 nm (LBH long). The optical system contains three electro-mechanical devices : an entrance aperture door, a filter wheel, and a folding mirror. The purpose of the entrance door is to close the instrument during non-operating conditions (integration, launch, thruster burns), and to protect it. Because this instrument is used at altitudes between two and nine earth radii (RE), the entrance door is exposed to bombardment by ionized particles and no buildup of electrostatic charge is allowed. Also, in the event it should fail in the closed position, it is designed to work as a broad passband window for the entire FUV region. Our research goal was to develop a conductive coating to meet the following specifications.

a) substrate : 3" diameter, 0.125" thickness MgF_2 window
b) transmittance : > 50 % for entire FUV region
c) resistance : < 10 kΩ/$\square$
d) should be stable chemically and mechanically

3. SEMICONDUCTOR MATERIALS

3.1. Conductivity

Oxide films, deposited by whatever means, appear to grow on oxide substrates as continuous films from the outset of deposition and do not have the island structure typically found in metal films. However, due to a smaller number of carriers compared to metal films, thicker films are required to achieve the same conductivity. Therefore, 200 nm to 400 nm thickness is usually required for semiconductor transparent conductive films in the visible and IR region.[4] For an antistatic film, less conductivity is required. Haas et. al.[5] achieved 700 Ω/$\square$ with 36 nm In_2O_3 film and 6 kΩ/$\square$ with 31 nm In_2O_3 +SnO_2 film for a space temperature control application.

The electrical properties of semiconductor films are very dependent on stoichiometry and the incorporation of impurities, either purposeful or inadvertent. Also they are relatively unstable, chemically, and depend on the fabrication parameters; fabrication process, starting material, substrate temperature, deposition rate, and annealing temperature and time. For nominally equivalent materials, even similar processes often result in quite different properties.

3.2. Transmittance

Previously reported studies about the optical properties of oxide semiconductor coatings have focused on the visible and IR regions where oxides have low absorption. The lowest wavelength reported was 200 nm. Hass et. al.[5] measured their In_2O_3 and In_2O_3 +SnO_2 coatings prepared by evaporation and sputtering down to this wavelength. They got 25% transmittance for a 36 nm In_2O_3 film and 23 % with a 31 nm In_2O_3 +SnO_2 film at 200 nm. Their spectral measurement results showed that there was less transmittance at the shorter wavelength.

Dobrowlski et. al.[4] reported optical constants of their ITO films (thickness 184 nm ~ 412 nm) formed by ion-assisted deposition down to a wavelength of 400 nm. At 400 nm, the absorption coefficients were 0.04 ~ 0.05, but increasing with a very steep gradient.

These prereported results showed that oxide semiconductors are very absorbing below 400 nm. Therefore, we need a very thin film to achieve the transmittance requirement.

3.3. Experimental results on the ITO coating

RF-sputtering was used to fabricate ITO coatings to test the possibility of using semiconductor antistatic films in the FUV region. ITO was selected as a trial material because it is reported to have the lowest resistance and the required conductivity could be achieved with minimum thickness. The sputtering target material was 99.99% {(In_2O_3)91% (SnO_2)9%} supplied by Angstrom Sciences. The initial vacuum was $4 \sim 5 \times 10^{-5}$ torr and the Ar gas flow inlet was set to reach a vacuum of 5×10^{-2} torr during the sputtering. The oxygen valve was kept closed and the substrate was not heated.

Before deposition onto the MgF_2 substrate, masked and unmasked Pyrex 1/2" substrates were used for testing. We used the masked Pyrex coating to measure the thickness with a Talystep profiler and found the deposition rate to be 8 nm/min. This deposition rate was used to control the thicknesses afterwards keeping the parameters the same except for deposition time. The unmasked Pyrex substrate was used to measure the square resistance by the method of reference 6. In a 4 minute sputtering time, we obtained 5.7 kΩ/□ resistance which is very similar to Hass et. al.'s[5] result.

32 nm and 64 nm coatings are deposited on 1/2" diameter and 0.125" thickness MgF_2 substrates for optical measurements. Our optical measurement system which is located at the NASA Marshall Space Flight Center is explained elsewhere.[7] The transmittance at normal incidence and the reflectance at a 6° angle of incidence are shown in Figure 1. The reflectance remained around 15% through the entire FUV region and the transmittance decreased monotonically to the short wavelength side. The absorption loss increases at shorter wavelengths. This result seems consistent with Hass et. al.'s[5] and Doborowalsky et. al.'s[4] results. It is evident that ITO is not a good material for transparent conductive coatings in the FUV region. With these disappointing results further experiments to change the deposition parameters were abandoned.
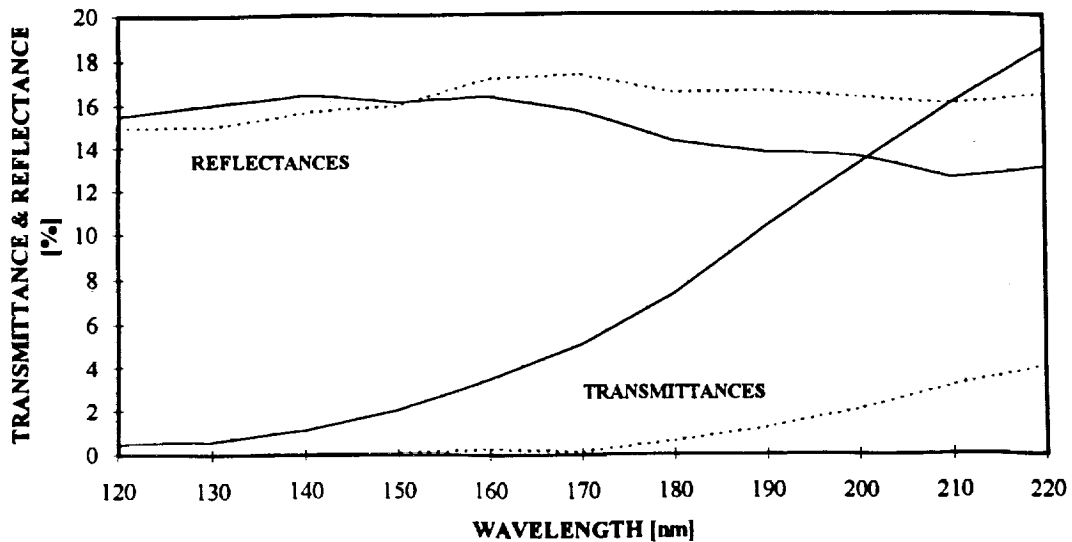
Figure 1. Measured transmittances and reflectances of 32 nm (solid lines) and 64 nm (dotted lines) ITO coatings on MgF$_2$ substrates.

4. METAL COATINGS

4.1. Conductivity

Metal films that have been studied for transparent conductive coating applications include : Au, Pt, Pd, Ag, Cu, Fe, and Ni.[1] However, Au is predominantly used.[8] Au is a noble metal that is chemically stable and has a very low electrical resistance.[9]

The most important factor for the conductivity of a thin metal film is island formation. Since, in nearly every case, metal atoms arrive with energies greater than kT (where T is the substrate temperature), it is found that some of the atoms reevaporate, some are directly reflected from the surface, and some lose their energy by moving about the substrate surface until a small cluster, or island, is formed at a site occupied by a nucleus. As the film gets thicker, there is a coalescence of the islands and a continuous film is obtained.

The implication of an island structure to transparent conductors is threefold.[1] First, the resistivity of such films is very high. Second, if the islands become quite large, they act to scatter incident light, rather than transmit it. Third, all other things being equal, a thicker film must be deposited to obtain sufficient electrical conductivity, but this results in more light absorption loss. Therefore, a thin continuous film material is better for this purpose than those materials which have lower bulk resistance.

Sennett and Scott[10] observed the structure of evaporated films of eight different metals in an electron microscope. They found that for Au and Ag, the thickness for which the aggregation began to merge was approximately 18 nm. With the resolution obtainable in their electron microscope, a Cr film

as thin as 2 nm appeared to be continuous. Therefore, we selected Cr as the best coating material to get a required conductivity with a minimum thickness.

4.2. Transmittance

We attempted to theoretically estimate the transmittance using the optical constants of metal coating materials found in references 11 and 12. The transmittance, reflectance, and absorptance can be calculated by the standard matrix method with known optical constants of the film and substrate and the thickness of the film.[13] The calculated transmittances for 2 nm thickness of Pt, Au, Pd, Ag and Cr films on MgF_2 substrates are shown in Figure 2. We used the optical constants for a MgF_2 substrate from reference 14. As we can see there is little difference in transmittance for candidate materials in the FUV region. The optical constants of our candidate materials do not differ very much over the entire FUV region. Therefore, the reflectances from the top surface of the film, assuming very thick films, are similar and the absorption loss plays the critical role in determining the transmittance. Apparently, the extinction coefficients (i.e. the imaginary part of optical constant) are all of the same order of magnitude.
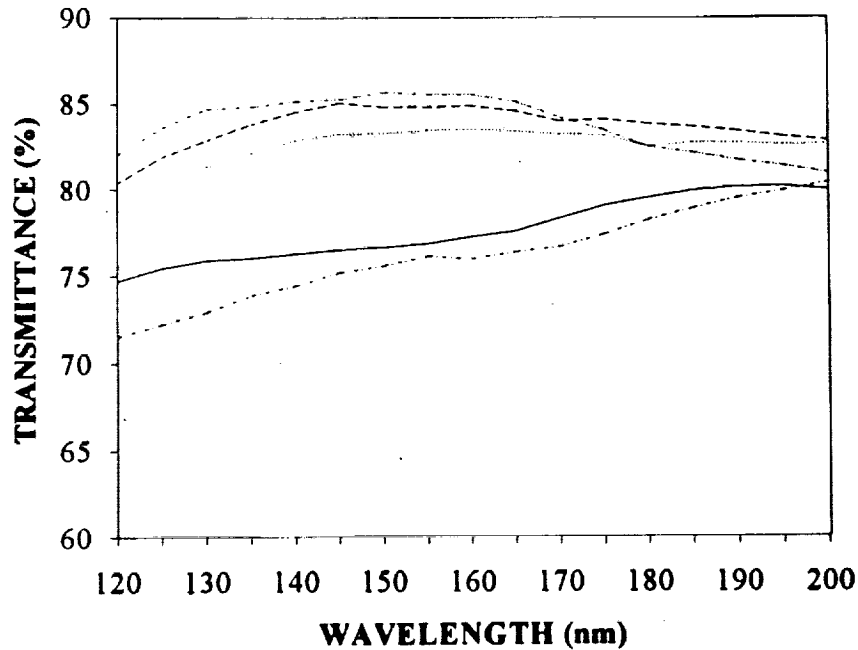
Figure 2. Calculated transmittances for the 2 nm thickness metal films on MgF_2 substrates : Pt (dashed and dotted line), Au (solid line), Pd (dotted line), Ag (dashed line), and Cr (dashed and double dotted line).

If we neglect the interference effect between multiple reflected waves in the thin film, the ratio of the transmitted light intensity I to the light intensity Io is given by the relation :

$$\frac{I}{I_o} = \exp(-\frac{4\pi}{\lambda}kd) \qquad (1)$$

Because the values of k are close to 1, the thickness, d, should be smaller than 6 nm to get $I/I_o > 0.5$ for a wavelength of 120 nm. Au and Ag are not suitable for our purposes.

4.3. Experimental results on the Cr coating

For reason explained in section 4.1, Cr was selected as our trial material. Cr is fairly inert chemically. Because of its high corrosion resistance, it has been vacuum evaporated to form mirrors on glass, used for electroplated or evaporated cathodes in Geiger counters with chemically active gas fillings, and as electrodeposited anti-corrosion layers for the external mountings of electron tubes.[9]

We deposited Cr by the evaporation method with an e-beam gun in a 2×10^{-5} torr vacuum. The source material was 99.9 % granulate type supplied by Balzers. In order to get good adhesion, the substrate was heated to 200 °C and the deposition rate was slow.(4 nm/min) Before deposition on the MgF$_2$ substrate, a Pyrex substrate was used to find the film thickness which satisfied the conductivity requirement. The thickness and deposition rate were monitored by a Quartz crystal monitor which was calibrated using the Talystep thickness profiler.

It was found that only a 1 nm thickness Cr coating had good conductivity, with 2.15 kΩ/□ of resistance. We monitored the change of the resistance of the Cr coating (thicknesses of 1 nm and 2 nm) which had been kept on a lab shelf without any special care. We measured the square resistance once a week for the first three months and once a month afterward. There has been no change in the resistance in 6 months. This also means that the coatings adhere so well that the probes for the resistance measurement do not make any serious scratches.

Figure 3 shows the transmittance measurements of the 1 nm and 2 nm Cr coatings. The transmittance of the 1 nm film satisfies the requirement but has a very low transmittance compared to the calculated transmittance. The reason can be explained by four possibilities. First, the optical constant we used from the reference is different from that of our coating material. Second, the coating is oxidized and has different properties than pure Cr. Third, the absorption of the substrate and the reflection from the bottom surface of the substrate are not included in the calculation. Fourth, scattering loss is not calculated.

5. SUMMARY

ITO and Cr thin film materials were tried as antistatic coatings for a FUV camera window.In the ITO case, at least a 32 nm thickness was required to achieve the desired resistance and it had a severe absorption loss so that it could not be used as a transparent conductive window material. Instead, Cr films were found to be good for this purpose. Only 1 nm film thickness was required to provide conductivity and the transmittance was higher than 50 % between the wavelengths of 123 nm and 220 nm. Our Cr coating did not show signs of aging or deterioration for six months and also had good mechanical adherence.

Figure 3. Measured transmittances of 1 nm (solid line) and 2 nm(dotted line)Cr coatings on MgF₂ substrates.

6. ACKNOWLEDGMENTS

7. REFERENCES

1. J. L. Vossen, "Transparent Conducting Films", in **Phys. Thin Films**, G. Hass, M. H. Francombe, and R. W. Hoffman eds. Vol. 9, pp. 1, Academic Press, New York, 1977.
2. L. Holland, **Vacuum Deposition of Thin Films**, pp. 491, Chapman & Hall, London, 1963.
3. D. G. Torr, M. R. Torr, M. Zukic, J. Spann, and R. B. Johnson, "The Ultraviolet Imager(UVI) for ISTP", in **Instrumentation for Planetary and Terrestrial Atmospheric Remote Sensing**, S. Chakrabarti ed., Proc. SPIE, Vol. 1745, pp. 61, 1992.
4. J. A. Dobrowolski, F. C. Ho, D. Menagh, R. Simpson, and A. Waldorf, "Transparent, conducting indium tin oxide films formed on low or medium temperature substrates by ion-assisted deposition", Appl. Opt., 26, 24, pp. 5204, 1987.
5. G. Hass, J. B. Heaney, and A. R. Toft, "Transparent electrically conducting thin films for spacecraft temperature control application", Appl. Opt., 18, 10, pp.1488, 1979.
6. M. Ohring, **The Materials Science of Thin Films**, chi. 10, Academic Press, Boston, 1992.

7. C. E. Keffer, M. R. Torr, M. Zukic, J. F. Spann, D. G. Torr, and J. Kim, "Radiation Damage Effects in Far Ultraviolet Filters and Substrates", in **Passive Materials for Optical Elements II**, G. W. Wilkerson ed. , Proc. SPIE, Vol. 2011, 1933.

8. H. K. Pulker, **Coating on Glass**, Ch. 6, Elsevier, Amsterdam, 1984.

9. W. Espe, **Materials of High Vacuum Technology, Vol. 1**, Pergamon Press, Oxford, 1966.

10. R. S. Sennett and G. D. Scott, "The Structure of Evaporated Metal Films and Their Optical Properties", J. Opt. Soc. Am., 40, 4, pp.203, 1950.

11. D. W. Lynch and W. R. Hunter, "Comments on the Optical Constants of Metals and an Introduction to the Data for Several Metals", in **Handbook of Optical Constants of Solids**, E. D. Palik ed., Academic Press, Orlando, 1985.

12. D. W. Lynch and W. R. Hunter, "An Introduction to the Data for Several Metals", in **Handbook of Optical Constants of Solids II**, E. D. Palik ed., Academic Press, Orlando, 1991.

13. M. Born, and E. Wolf, **Principles of Optics**, 6th ed., ch. 1, Pergamon, Oxford, 1980.

14. M. Zukic, D. G. Torr, J. F. Spann, and M. R. Torr, "Vacuum ultraviolet thin films 1: Optical constants of BaF_2, CaF_2, LaF_3, MgF_2, Al_2O_3, HfO_2, and SiO_2 thin films", Appl. Opt., 29, pp. 4284, 1990.